

# Magnesium Isotopic Composition of Interplanetary Dust Particles

Tezer M. Esat, D. E. Brownlee, D. A. Papanastassiou  
G. J. Wasserburg

There has been considerable interest in the nature and sources of interplanetary dust for many years. A prominent manifestation of interplanetary dust, the zodiacal glow, is due to scattered sunlight from a dust cloud concentrated in the plane of the ecliptic. Individual dust particles have lifetimes only on the order of  $10^4$  years. Destruction mechanisms in-

fraction consists of particles larger than  $10\text{ }\mu\text{m}$  (2).

Major advances have been made in collecting and identifying interplanetary dust particles (3). The dust particles are collected on air sampling surfaces flown on NASA U-2 aircraft at an altitude of 20 kilometers. Techniques for handling particles as small as  $5\text{ }\mu\text{m}$  and for determin-

**Summary.** The magnesium isotopic composition of some extraterrestrial dust particles has been measured. The particles are believed to be samples of interplanetary dust, a significant fraction of which originated from the disaggregation of comets and may contain preserved isotopic anomalies. Improvements in mass spectrometric and sample preparation techniques have made it possible to measure the magnesium isotopic composition of the dust particles, which are typically 10 micrometers in size and contain on the order of  $10^{-10}$  gram of magnesium. Of the 13 samples analyzed, nine have the terrestrial magnesium isotopic composition within 2 parts per thousand, and one shows isotopic mass fractionation of 1.1 percent per mass unit. A subset of the particles, described as chondritic aggregates, are very close to normal isotopic composition, but their normalized isotopic ratios appear to show nonlinear effects of 3 to 4 parts per thousand, which is near the present limit of detection for samples of this size. The isotopic composition of calcium was also determined in one particle and found to be normal within 2 percent. It is clear that the isotopic composition of interplanetary dust particles can be determined with good precision. Collection of dust particles during the earth's passage through a comet tail or an intense meteor stream may permit laboratory analysis of material from a known comet.

clude erosion due to collisions and sputtering by solar wind particles, as well as spiraling-in due to the Poynting-Robertson effect. The cloud is maintained in a quasi-steady state by injection of fresh material from comets, asteroids, and the interstellar medium (1). Interplanetary dust particles micrometers in size enter the earth's atmosphere without melting, with a flux roughly of the order of  $\sim 10^{-5}$  particle per square meter per second for particles  $10\text{ }\mu\text{m}$  or larger. A significant

ing their morphological and chemical characteristics have been developed (4). The extraterrestrial nature of these particles has now been well established, and they can be readily distinguished from terrestrial contaminants. Individual dust grains from the U-2 collections are in the size range 2 to  $50\text{ }\mu\text{m}$ , with masses typically of the order of  $10^{-9}$  gram. At present, the world's laboratory supply of this material is about  $10^{-6}$  g. The small amount of material available has permitted morphological and chemical characterization but, until now, has precluded the measurement of isotopic compositions, as standard sample preparation and mass spectrometric techniques are inadequate for isotopic measurements on individual grains weighing only  $\sim 10^{-9}$  g.

The isotopic composition of small samples in some cases can be measured with the ion microprobe; however, the accuracy obtained has been in the percent range and there are substantial uncertainties because of the large number of molecular interferences and uncontrolled mass fractionation effects in the sputtering process (5).

The recently discovered isotopic anomalies in the calcium- and aluminum-rich high-temperature inclusions in the Allende meteorite show that variations in isotopic abundances, presumably dating back to an isotopically heterogeneous solar nebula, have been preserved in some meteorites. Two, so far unique, inclusions from this meteorite are isotopically anomalous in almost every element studied (6, 7). In addition, remains of now extinct  $^{26}\text{Al}$  have been found in Al-rich phases as excesses in  $^{26}\text{Mg}$  (8, 9). Magnesium isotopic anomalies have also been found in the meteorites Leoville (10) and Murchison (11). It is clear that the isotopic imprints of nucleosynthetic sources that contributed to the material from which the solar system formed have not been completely obliterated; the record has been preserved in some meteorites.

Interplanetary dust grains constitute a distinct class of solar system materials that may contain preserved isotopic effects. There is considerable evidence that a significant fraction of interplanetary dust originated from the gradual disaggregation of short-period comets (12). The existence of comet dust tails is proof that comets are copious producers of dust. The correlation of meteor showers with comets and the similar orbital parameters of sporadic meteors and short-period comets suggest that comets are a significant and possibly the major source of interplanetary dust particles in the solar system (1). Studies of the luminosity and deceleration of some meteor streams in the earth's atmosphere indicate that some dust particles are fluffy objects of low density ( $\sim 1\text{ g per cubic centimeter}$ ). The precise isotopic analysis of cometary material is of particular interest because comets are believed to have aggregated at low temperatures at the outer fringes of the solar nebula and therefore may contain early solar system aggregates, condensates, or possibly presolar grains that were not vaporized during the formation of the solar system. Considering the isotopic anomalies recently discovered in meteorites, samples of cometary material are prime candidates for a search for the solar nebula's original, and evidently heterogeneous, isotopic composition. This information

T. M. Esat is a research fellow in the Kellogg Radiation Laboratory, California Institute of Technology (Caltech), Pasadena 91125. D. E. Brownlee is a research associate in the Division of Geological and Planetary Sciences at Caltech and an associate professor in the Department of Astronomy, University of Washington, Seattle 98195. D. A. Papanastassiou is a research associate and G. J. Wasserburg is a professor in the Division of Geological and Planetary Sciences at Caltech.

can provide new insights into the formation and evolution of the solar nebula and the nature of the sources of nucleosynthetic products. Because of the importance of this problem, we have developed improved methods for isotopic analysis of microscopic particles. These techniques were applied to the magnesium isotopic analysis of selected interplanetary dust particles (IDP's).

## Experimental Procedures

In this article we present magnesium isotopic data for 13 IDP's ranging in size from 10 to 30  $\mu\text{m}$ . The major element composition of IDP's consists of Si, Fe, Mg, S, O, and C, which comprise more than 90 percent of the total mass, with lesser amounts of Na, Al, Ca, Ti, Ni, and Cr. The main difficulty in the isotopic analysis of the available IDP's is that a typical 10- $\mu\text{m}$  particle contains only about 100 to 200 picograms ( $1 \text{ pg} = 10^{-12} \text{ g}$ ) of a major element such as Mg. Chemical separation is impractical because the amount of Mg introduced by contamination in the separation procedures is at least a factor of 10 higher than the Mg content of the sample. The direct-loading technique developed for the analysis of lead in  $10^{-11} \text{ g}$  quantities (13) and for Mg (14, 15) is much more suitable for the analysis of microscopic samples. Previous experiments have established that individual crystals directly placed on a filament and embedded in a matrix of silica gel treated with  $\text{H}_3\text{PO}_4$  acid can be used as thermionic sources in a mass spectrometer and yield stable beams of Mg for precise isotopic analysis. The direct-loading technique has been used to analyze single crystals as small as 20  $\mu\text{m}$  containing  $10^{-9} \text{ g}$  of Mg. The ionization efficiency for Mg (singly ionized Mg at the collector divided by total Mg on the filament) was estimated to be  $10^{-4}$  (15). For a 100-pg Mg sample, this corresponds to a mean current of  $\sim 10^{-14}$  ampere (for  $\sim 1$  hour) and is close to the noise level of the amplifier system for a simple Faraday cup. Major improvements in the blank levels and in the ionization efficiency for the directly loaded samples were required for the present work before reliable isotopic analyses could be undertaken for Mg samples as small as 50 pg with a precision of a few parts in a thousand.

After the IDP's were collected on U-2 flights, the samples were processed at University of Washington laboratories and then transferred to our laboratory, where further morphological and chemical analyses were undertaken. After

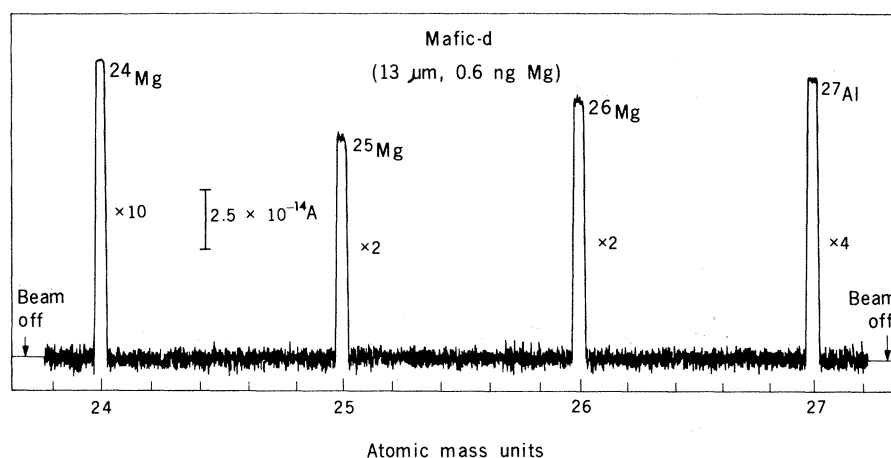


Fig. 1. Continuous scan of the Mg mass spectrum on the mass spectrometer Faraday collector for mafic particle d (see Table 4). The  $^{24}\text{Mg}$  signal is  $1.3 \times 10^{-12} \text{ A}$ . The bar marked  $2.5 \times 10^{-14} \text{ A}$  is the sensitivity corresponding to the base line. The spectral lines were scanned with a decrease in sensitivity by the factors indicated.

these studies the samples were prepared for mass spectrometric analysis. The particles were handled dry, using electrolytically etched tungsten needles with tips 5  $\mu\text{m}$  in diameter. The first three particles were loaded into our standard V-shaped rhenium filaments, 3 millimeters long and about 0.4 millimeter deep. In order to decrease the amount of Mg due to laboratory contamination and possibly improve the ionization efficiency, a new type of filament was prepared. This consisted of a hemispherical dimple 200  $\mu\text{m}$  in diameter pressed into flat Re filaments. The filaments were loaded by using a special mounting and heating fixture attached to an X-Y stage under a microscope. Before a sample was loaded, the dimple was filled with  $\sim 50 \mu\text{g}$  of silica gel and  $\text{H}_3\text{PO}_4$  acid from a microsyringe attached to a micromanipulator. To improve the adhesion of silica gel to the Re, trace amounts of glucose and citric acid solution (Tera "orange juice") were added. The grains were transferred from a glass microscope slide into the dimple with the tungsten needle attached to the micromanipulator. The particle was at all times in view under a microscope and the delivery and immersion of the particle into the wet silica gel- $\text{H}_3\text{PO}_4$  mixture could be positively verified. The sample was then fused with the silica gel- $\text{H}_3\text{PO}_4$  mixture and analyzed in the mass spectrometer.

For a typical IDP sample a  $^{24}\text{Mg}$  beam greater than  $10^{-12} \text{ A}$  could be sustained for more than 2 hours. The ionization efficiency for Mg achieved with the dimple filament is  $\sim 10^{-2}$ , which represents a factor of 100 improvement in the sensitivity of the direct-loading technique. A mass spectrum obtained for a typical IDP is shown in Fig. 1. Except for Mg, the only other peak in the region of inter-

est is the  $^{27}\text{Al}$  peak, which was sufficiently weak for all IDP analyses that no scattered  $^{27}\text{Al}$  background was detectable in the mass 24 region ( $< 2 \times 10^{-15}$  amperes). For each sample analyzed, the data consisted of 150 to 250 individual ratio determinations from isotope measurements obtained in the cyclic order  $^{24}\text{Mg}$ - $^{25}\text{Mg}$ - $^{26}\text{Mg}$ - $^{24}\text{Mg}$ .

## Contamination

To test the procedures in the modified direct-loading technique and determine the beam stability and intensity obtainable from samples with a Mg content on the order of 100 pg, terrestrial olivine grains (with normal isotopic composition) and spinel and pyroxene crystals from the anomalous Allende inclusions EK1-4-1 and C-1 were analyzed. The data on the Allende samples are particularly useful because EK1-4-1 is fractionated by +20 per mil per mass unit and C-1 by 30 per mil per mass unit. Any contamination with Mg of terrestrial isotopic composition in the processing of EK1-4-1 and C-1 samples would result in a lower measured fractionation. For example, for C-1 a 33 percent addition of terrestrial Mg would reduce the measured fractionation from 30 to 20 per mil per mass unit. In addition, after normalization for mass-dependent fractionation, EK1-4-1 and C-1 have a deficiency in the  $^{26}\text{Mg}/^{24}\text{Mg}$  ratio with  $\delta^{26}\text{Mg} = -3.4$  and  $-1.8$  per mil, respectively (6). Therefore, analyses of small crystals from these samples can be used as indicators of overall laboratory contamination and of the resolution to be achieved in determining isotopic effects.

Magnesium contamination was also determined independently by using a

Table 1. Magnesium contamination determined by use of a  $^{25}\text{Mg}$  tracer.

Method	Mg contaminant (pg)
Total procedure	1.5
	3.6
	3.5
Excess glucose-citric acid mixture*	3.8
Tungsten needle†	7.1

\*The amount used was 20 times the normal amount. †The tip of the needle was heated in a dimple containing silica gel and  $\text{H}_3\text{PO}_4$ .

tracer solution with a known content of separated  $^{25}\text{Mg}$ . In this case, a procedural blank was measured by repeating every step in the processing and loading of small crystals except that a measured amount of the  $^{25}\text{Mg}$  tracer solution was substituted for the actual crystal. Magnesium blanks were also determined for the glucose-citric acid mixture and the tungsten needle tip. The data for the various blank determinations are listed in Table 1 and the results are summarized below.

With the  $^{25}\text{Mg}$  tracer, (i) the total measured procedural blank ranged from 2 to 4 pg; (ii) addition of excessive glucose-citric acid mixture had an insignificant effect on the Mg blank; and (iii) prolonged heating of the tungsten needle in the silica gel- $\text{H}_3\text{PO}_4$  mixture introduced roughly as much Mg as in the total blank. However, contact between the needle and the filament in the actual loading of crystals is minimal and takes place at room temperature.

With the C-1 samples, small (6 to 13

$\mu\text{m}$ ) spinel and pyroxene grains were characterized in a scanning electron microscope (SEM) and their volumes were determined. The data are shown in Table 2, where the column labeled "fractionation" represents the fractional deviation of the directly measured average  $^{25}\text{Mg}/^{24}\text{Mg}$  ratio for the sample from the grand mean value of  $^{25}\text{Mg}/^{24}\text{Mg} = 0.12475$  for terrestrial samples (8). The  $\delta^{26}\text{Mg}$  column represents the fractional deviation of the  $^{26}\text{Mg}/^{24}\text{Mg}$  ratio from the terrestrial value of 0.139805 after correction for mass-dependent fractionation by use of the measured  $^{25}\text{Mg}/^{24}\text{Mg}$  ratio (see footnote in Table 2). Inherent fractionation effects ( $\Delta$ ) appear as nonzero entries in the fractionation column, and any nonlinear effects (such as excess  $^{26}\text{Mg}$  from  $^{26}\text{Al}$  decay or anomalous nuclear components at mass 24, 25, or 26) appear as nonzero entries in the  $\delta^{26}\text{Mg}$  column.

The first two entries in Table 2 are for pyroxene grains, which were relatively large ( $\approx 10 \mu\text{m}$ ) and contained roughly 100 pg of Mg. Within errors, there is no shift from the expected fractionation value of 30 per mil per mass unit. The next three grains analyzed were spinels with Mg contents of 80, 60, and 20 pg, respectively. Within the errors, the fractionation data for these grains also show no effects due to contamination. An upper limit can be estimated from the uncertainties in the analysis of the smallest grain. For a fractionation value as low as 24.5 per mil we obtain a blank limit of 3 pg, which is consistent with the blank determined with the  $^{25}\text{Mg}$  tracer. The technique of using EK1-4-1 and C-1 cannot be applied to even smaller samples be-

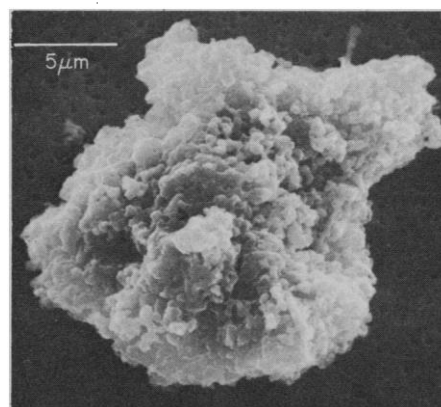


Fig. 2. Scanning electron micrograph of a chondritic aggregate consisting of many individual grains in a fluffy porous structure (particle d in Table 4).

cause of the diminishing signal levels and corresponding decrease in the precision of the data. For the 6- $\mu\text{m}$  spinel (20 pg of Mg), the  $2\sigma$  (2 standard deviations) mean error determined for the fractionation value is at the 10 per mil level. The smallest Mg content of the IDP's analyzed was about 100 pg, and the Mg blank contribution for this worst case is less than 5 percent. The blank levels obtained previously for directly loaded samples were of the order of 50 pg (15)—a factor of 10 higher than the present levels.

### Resolution of Isotopic Effects

The analyses of crystals from the Allende inclusions C-1 and EK1-4-1 as well as the repeat analyses of terrestrial samples show that the expected fractionation effects are well resolved for samples as small as 100 pg. Differences in fractionation of 5 per mil per mass unit are clearly resolvable. By comparison, for larger samples the resolution in fractionation is 2 to 3 per mil per mass unit (8).

The EK1-4-1 samples have a nonlinear effect of -3.4 per mil in  $\delta^{26}\text{Mg}$  and provide a test for the precision obtainable when the direct-loading technique with the dimple filament is used for Mg amounts of the order of  $10^{-10}$  g. However, in contrast to IDP's, EK1-4-1 crystals have substantial amounts of  $^{27}\text{Al}$ , which result in high  $^{27}\text{Al}$  signals and a reflected  $^{27}\text{Al}$  beam under the  $^{24}\text{Mg}$  peak (15). Extensive tests have shown that the reflected beam results in about a -1.5 per mil offset in the  $\delta^{26}\text{Mg}$  value, essentially independent of the intensity of the  $^{27}\text{Al}$  beam beyond a certain threshold. At this level of precision the fractionation effects do not seem to be affected by the high  $^{27}\text{Al}$  beam. Results of isotopic analyses of EK1-4-1 spinel grains are listed in

Table 2. Magnesium contamination and sensitivity to nonlinear effects for individual crystals.

Sample	Size* ( $\mu\text{m}$ )	Mg content† ( $10^{-12}$ g)	Fractionation‡ $\Delta(^{25}\text{Mg}/^{24}\text{Mg}) \pm 2\sigma$ (per mil)	Mg blank§ ( $10^{-12}$ g)	$\delta^{26}\text{Mg} \pm 2\sigma$ ¶ (per mil)
Allende inclusions					
C-1 pyroxene	10	100	$29 \pm 1$		$-1.1 \pm 2.5$
	13	130	$28 \pm 1$	4	$-2.0 \pm 2.8$
C-1 spinel	9	80	$30 \pm 1$		$-2.3 \pm 3.0$
	8	60	$31 \pm 1$		$-2.2 \pm 2.5$
	6	20	$34 \pm 9$	3	$-3 \pm 20$
EK1-4-1 spinel	22	1000	$20 \pm 1$		$-3.5 \pm 2.0$
	13	160	$19.5 \pm 0.4$		$-3.7 \pm 0.6$
	11	100	$18.9 \pm 0.4$		$-3.4 \pm 0.6$
	10	75	$19.6 \pm 0.5$		$-3.9 \pm 0.8$
Terrestrial standards#			$0 \pm 2$		$0 \pm 2$

\*Typical crystal dimension were determined from the SEM image. †The Mg content was estimated from the volume of each crystal. ‡ $\Delta(^{25}\text{Mg}/^{24}\text{Mg}) = [(^{25}\text{Mg}/^{24}\text{Mg})_{\text{M}}/0.12475 - 1] \times 10^3$  where M denotes the raw measured ratio and  $^{25}\text{Mg}/^{24}\text{Mg} = 0.12475$  is the grand mean value for terrestrial samples used for normalization. The corresponding grand mean value for raw measured  $^{25}\text{Mg}/^{24}\text{Mg}$  is 0.13569. §Upper limit calculation from C-1 with  $\Delta(^{25}\text{Mg}/^{24}\text{Mg})_{\text{avg}} = 30 \pm 2$  per mil. ¶Corrected (c) for fractionation according to  $(^{26}\text{Mg}/^{24}\text{Mg})_{\text{c}} = (^{26}\text{Mg}/^{24}\text{Mg})_{\text{M}}/\alpha^2$ , where  $\alpha = (^{25}\text{Mg}/^{24}\text{Mg})_{\text{M}}/0.12663$ ; the normal (N)  $(^{25}\text{Mg}/^{24}\text{Mg})_{\text{N}} = 0.12663$  is that reported by Catanzaro and Murphy (22). # $\delta^{26}\text{Mg} = [(^{26}\text{Mg}/^{24}\text{Mg})_{\text{c}}/0.139805 - 1] \times 10^3$ . The value 0.139805 is obtained by correction for fractionation of the grand mean for the raw measured  $^{26}\text{Mg}/^{24}\text{Mg} = 0.13569$  for terrestrial samples. A bias of +1.5 per mil was added to  $\delta^{26}\text{Mg}$  for each sample of EK1-4-1 and C-1 because of the presence of a reflected  $^{27}\text{Al}$  beam during analysis of these samples. #Directly loaded olivine crystals.

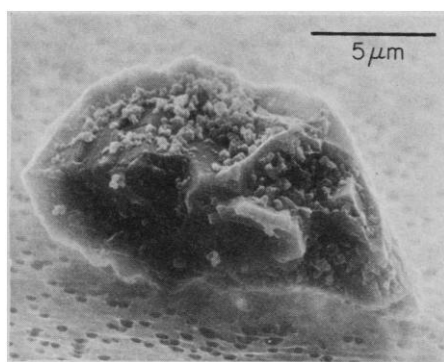


Fig. 3. Scanning electron micrograph of a mafic IDP. The particle consists of a single crystal of forsteritic olivine covered with fine-grained debris. The chemical composition of the surface debris is chondritic and is similar in morphology to the chondritic aggregate in Fig. 2.

Table 2; a +1.5 per mil bias was added to the measured  $\delta^{26}\text{Mg}$  value for these samples. It is evident that for samples with 100 to 200 pg of Mg the expected  $\delta^{26}\text{Mg}$  value can be reasonably well reproduced in all cases. This shows that isotopic anomalies of the order of 3 to 4 per mil can be resolved, with the present techniques, for samples as small as 100 pg. In contrast, the analyses of C-1 samples (Table 2) show that the present techniques are not precise enough to resolve the -1.8 per mil shift in  $\delta^{26}\text{Mg}$ , as the errors are of the same order as the magnitude of the effect. We note that the +1.5 per mil correction was applied only to the C-1 and EK1-4-1 samples that showed high  $\text{Al}^+/\text{Mg}^+$  ratios during mass spectrometer runs; no such corrections were applied for the other analyses reported here.

### Description of the Interplanetary

#### Dust Particles

The particles were collected on plates covered with a thin layer of viscous silicone oil. Before isotopic analysis the particles were washed with xylene or hexane to remove traces of silicone oil, handled with glass and tungsten needles, and coated with palladium films 100 angstroms thick. All of the particles were characterized optically and with an SEM equipped with an energy-dispersive x-ray detector. X-ray diffraction patterns were obtained for a few particles, using a 28.6-mm Debye-Scherrer vacuum camera. The particles analyzed can be grouped into three categories—chondritic aggregates, mafic particles, and spheres—based on morphology and on elemental and mineralogical composition. The three types are briefly described below.

*Chondritic aggregates.* These com-

prise the bulk of the extraterrestrial micrometeorites recovered from the U-2 collection plates. They are black, opaque aggregates of amorphous material and grains ranging in size from less than 100 Å to several micrometers. A typical 10-μm particle contains more than 1 million submicrometer grains in a loosely bound structure that is highly porous for some particles and compact for others. Transmission electron microscope studies of crushed particles reveal that some of the submicrometer grains are single minerals, while others are themselves aggregates of grains smaller than 50 Å embedded in amorphous material. The fine-scale structures of typical IDP chondritic aggregates are morphologically distinct from the crumpled fibrous matrix material observed in C1 and C2 carbonaceous chondrites (16). However, the elemental abundance of these IDP aggregate particles is chondritic—that is, they contain Si, Mg, Fe, S, Na, Al, Ca, Ni, Cr, and Mn in proportions similar to those found in chondritic meteorites (see Table 3). They are thus called “chondritic aggregates” based on this chemical similarity, although they do not appear to be samples of typical chondrites. A representative sample consisting of several chondritic aggregates was analyzed for  $^4\text{He}$  content (17), and some were found to have large concentrations of solar wind  $^4\text{He}$ . The high  $^4\text{He}$  retention together with the loosely compacted and fragile appearance is evidence against significant heating during atmospheric entry and rules out their being meteoritic ablation fragments. An SEM image of a chondritic aggregate particle analyzed for Mg isotopic composition is shown in Fig. 2.

*Mafic particles.* The particles in this category were selected because they were largely monomineralic and because of their greater size and Mg content. They are either single crystals or poly-

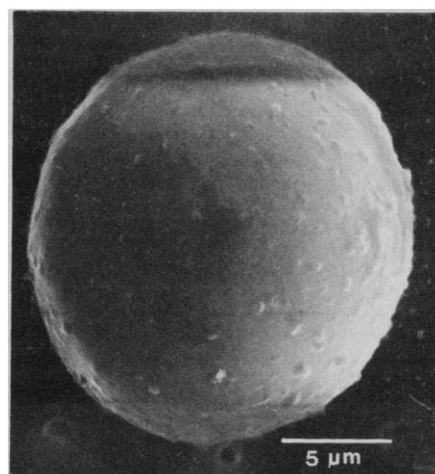


Fig. 4. Scanning electron micrograph of a spherical IDP. The Mg analysis of this particle showed an isotopic fractionation of 11 per mil per mass unit. The spheres are enriched in Mg, Al, and Ca relative to other types of IDP's. The surface blebs on this specimen are free of adhering matter except for some that are enriched in iron.

crystalline aggregates of grains several micrometers in size, often of forsteritic olivine. The particles are transparent, but many have clumps of micrometer and submicrometer opaque grains adhering to their surfaces. The chemical composition of these clumps is chondritic. Most of the particles are either forsteritic olivine or enstatite, although one particle is apparently a mixture of olivine and calcium-rich pyroxenes and is covered with nickel-rich troilite. Mineral phases are inferred on the basis of chemical composition as determined by the SEM analysis. These mafic particles differ considerably in composition from the more common IDP's, which typically are

Table 3. Chemical composition (ratio by weight, relative to Si) of interplanetary dust particles.

Element	Chondritic aggregate*	Mafic particle†	Sphere‡	C1 chondrites§	
				Bulk	Matrix
Na	0.04	0.16	0.03	0.10	0.013
Mg	0.74	0.68	1.33	0.89	0.80
Al	0.06	0.04	0.17	0.10	0.09
Si	1.00	1.00	1.00	1.00	1.00
S	0.40	0.15	0.003	0.53	0.15
K	0.01	0.01		0.01	0.015
Ca	0.07	0.07	0.26	0.10	0.015
Ti			0.01	0.005	0.002
Cr	0.02	0.04		0.019	0.022
Mn	0.03	0.02		0.017	0.009
Fe	1.25	1.19	0.01	1.72	1.07
Ni	0.08	0.04		0.09	0.10

\*Average composition for thirteen particles reported by Brownlee (3).

†Chemical composition of mafic particle e in Table 4.

‡Chemical composition of sphere a in Table 4.

§Mean composition of C1 carbonaceous chondrites in bulk and for the fine-grained matrix material, from McSweeney and Richardson (20).

rial similar to either the carbonaceous chondrite matrix or the slightly different material that composes the more common chondritic aggregates. An SEM image of a typical mafic particle is shown in Fig. 3. The elemental composition of a mafic particle that is a polycrystalline aggregate is given in Table 3.

**Spheres.** Rare spheres of enigmatic

origin have been consistently collected during the entire U-2 air sampling program. The spheres are not of chondritic composition and do not contain surficial chondritic debris. Relative to chondritic abundances, they are enriched in Mg, Ca, Al, and Ti by factors of as much as 3 and depleted in sulfur (Table 3). Of the three spheres analyzed, two were trans-

parent and had very low iron contents; the third was black and contained iron in roughly chondritic abundance. The iron-rich sphere contained several micrometer-sized magnetite grains. An SEM image of one of the spheres analyzed is shown in Fig. 4. The spheres may be meteor ablation particles, objects produced in space, or terrestrial particles, although because of their large fall speeds, 10- $\mu$ m terrestrial particles are exceedingly rare in the stratosphere. The only contaminants that are similar in morphological character in the U-2 collections are aluminum oxide spheres produced in solid-fuel rocket exhaust, but these are rarely as large as 10  $\mu$ m (18).

Representative results of chemical analyses for each type of IDP are shown in Table 3. The data were obtained by quantitative energy-dispersive x-ray analyses. Spectral line areas were determined by a least-squares fit to standards. Elemental abundances were computed relative to silicon by using the Armstrong-Buseck particle program (19), which performs absorption, fluorescence, and atomic number corrections for unsectioned particles. The IDP's contain significant amounts of oxygen and carbon which cannot be detected by x-ray analyses. The mean chemical compositions of the bulk and the fine-grained matrix of CI carbonaceous meteorites (20) are given in Table 3 for comparison.

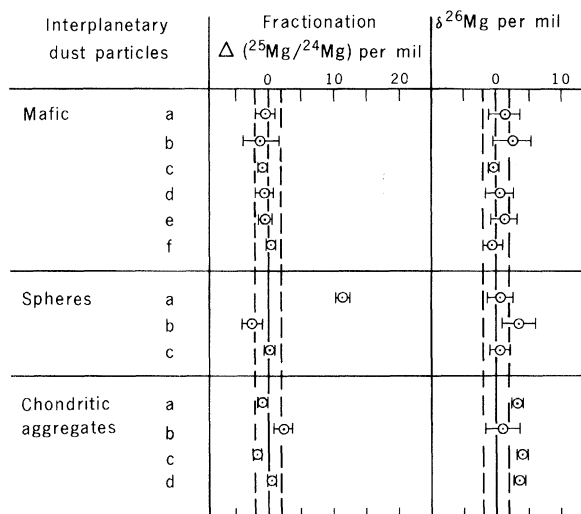


Fig. 5. Magnesium isotopic composition of the IDP's. Fractionation and  $\delta^{26}\text{Mg}$  are explained in Table 2. Bands of  $\pm 2$  per mil around the  $\Delta(^{25}\text{Mg}/^{24}\text{Mg}) = 0$  and  $\delta^{26}\text{Mg} = 0$  axes represent the resolution limits for the direct-loading techniques described here. The sphere shows large mass fractionation but no nonlinear effect. The chondritic aggregate analyses fall slightly to the right of the  $\delta^{26}\text{Mg} = \pm 2$  per mil band.

Table 4. Magnesium isotopic composition of interplanetary dust particles, lunar orange and green glass, and terrestrial standards. Column headings are explained in Table 2.

Sample*	Size ( $\mu\text{m}$ )	Mg content ( $10^{-9}$ g)	Fractionation $\Delta(^{25}\text{Mg}/^{24}\text{Mg}) \pm 2\sigma$ (per mil)	$\delta^{26}\text{Mg} \pm 2\sigma$ (per mil)
<b>Interplanetary dust particles</b>				
<b>Mafic particles</b>				
a	22	4.5	$-0.8 \pm 1.4$	$1.7 \pm 2.3$
b	12	1	$-1.2 \pm 2.8$	$2.6 \pm 3.1$
c	23	3	$-0.9 \pm 0.4$	$-0.6 \pm 0.4$
d	13	0.6	$-0.7 \pm 1.1$	$0.3 \pm 2.3$
e	20	0.5	$-0.6 \pm 0.9$	$1.4 \pm 2.0$
f	10	0.1	$0.3 \pm 0.7$	$-0.5 \pm 1.6$
<b>Spheres</b>				
a	10	0.1	$11.3 \pm 0.9$	$0.5 \pm 2.0$
b	11	0.1	$-2.7 \pm 1.5$	$3.5 \pm 2.5$
c	16	0.3	$0.3 \pm 0.8$	$0.6 \pm 1.5$
<b>Chondritic aggregates</b>				
a	20	0.4	$-0.8 \pm 0.6$	$3.2 \pm 1.1$
b	15	0.2	$2.2 \pm 1.3$	$1.0 \pm 2.8$
c	30	0.8	$-1.9 \pm 0.5$	$4.0 \pm 0.8$
d	20	0.4	$0.5 \pm 0.7$	$3.5 \pm 1.1$
<b>Lunar orange glass</b>				
a	15	0.6	$0.5 \pm 0.9$	$0.0 \pm 2$
b	30	5	$-1.7 \pm 0.4$	$0.1 \pm 0.6$
<b>Lunar green glass</b>				
a	80	95	$-2.0 \pm 0.2$	$-2.0 \pm 0.2$
b	70	60	$-0.5 \pm 0.6$	$-1.2 \pm 0.5$
c	100	190	$1.7 \pm 0.2$	$-1.7 \pm 0.2$
d†	180	150‡	$0.1 \pm 0.1$	$-0.6 \pm 0.2$
e†	170	150‡	$0.5 \pm 0.2$	$0.2 \pm 0.3$
f†	200	130‡	$0.6 \pm 0.2$	$-0.7 \pm 0.2$
g†	210	130‡	$1.1 \pm 0.2$	$-0.5 \pm 0.2$
<b>Terrestrial olivine standards</b>				
a	20	4	$0.8 \pm 0.9$	$-0.2 \pm 1.5$
b	18	3	$-1.0 \pm 0.8$	$-0.4 \pm 1.6$
c	80	180	$1.4 \pm 0.1$	$-0.3 \pm 0.2$

\*All the samples, unless otherwise indicated, were directly loaded.  
‡Amount of Mg loaded on filament.

†Chemically separated samples.

## Results for Interplanetary Dust Particles

The Mg isotopic data for IDP's, grouped according to morphological type, are shown in Table 4 and Fig. 5. We looked for two distinct types of effects—mass fractionation and nonlinear isotopic anomalies. The raw values of the average  $^{25}\text{Mg}/^{24}\text{Mg}$  were used to calculate a fractionation value for each experiment. The dashed lines in Fig. 5 represent a  $\pm 2$  per mil band for shifts in  $^{25}\text{Mg}/^{24}\text{Mg}$ , and we believe that any fractionation effects within this band are not significant as they reflect the range of instrumental fractionation effects. Considering the small sample sizes for all of the IDP's analyzed, as well as the fact that only a single analysis could be done for each particle, anomalous isotopic effects have to be larger than a few per mil to be detected. In general, the quality of the data may vary depending on the ion beam intensity and stability during a particular analysis. The experiments with EK1-4-1 spinels described in the previous section show that effects of 3 to 4 per mil can be clearly resolved for the better runs with uncertainties of  $\sim \pm 0.6$

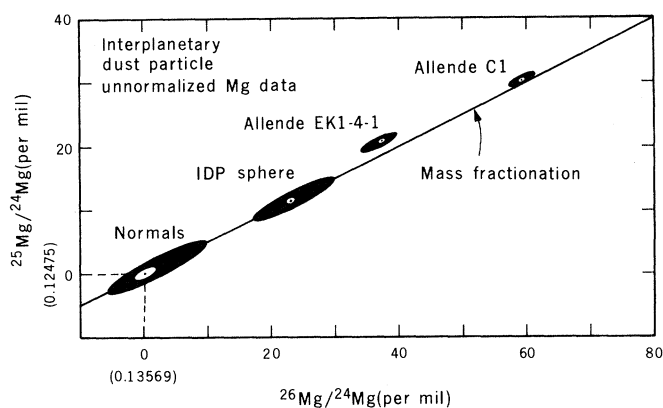
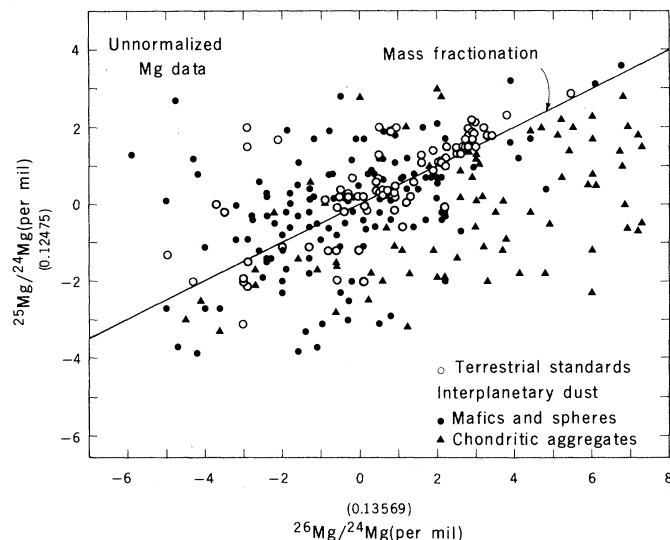


Fig. 6 (left). Correlation of  $^{25}\text{Mg}/^{24}\text{Mg}$  versus  $^{26}\text{Mg}/^{24}\text{Mg}$  for terrestrial standards, the fractionated IDP sphere, and the fractionated Allende inclusions EK1-4-1 and C-1. The IDP sphere shows a large displacement from the terrestrial samples along the fractionation line. Two Allende samples are slightly off the fractionation line, which is consistent with their distinct nonlinear effects superimposed on large mass fractionation. Large black ellipses are the error envelopes representing the means of ten individual ratios for all data sets (6). The small open ellipses represent the  $2\sigma$  mean error envelopes of the grand means of each experiment. Fig. 7 (right). Correlation diagram of  $^{25}\text{Mg}/^{24}\text{Mg}$  versus  $^{26}\text{Mg}/^{24}\text{Mg}$  for all the data obtained on subnanogram Mg samples (except for the highly fractionated sphere). Each point represents the mean of ten individual ratios. All the data lie in an envelope bounded by  $^{25}\text{Mg}/^{24}\text{Mg} = \pm 3.5$  per mil and  $^{26}\text{Mg}/^{24}\text{Mg} = \pm 7$  per mil along a mass fractionation line of slope 0.5 through terrestrial normal Mg. The data for the chondritic aggregates are offset downward or to the right of the fractionation line.



per mil. The  $\pm 2$  per mil band bracketing  $\delta^{26}\text{Mg} = 0$  in Fig. 5 represents a reasonable limit beyond which anomalous effects can be distinguished, depending on the precision of the data. The isotopic results are described below for each morphological type.

**Mafic crystals.** These were chosen primarily for their size and single-crystal nature. Six of these particles had Mg contents ranging from 0.1 to 4.5 nanograms. The first three particles listed in Table 4 were analyzed on Re V-shaped filaments with lower sensitivity and consequently show larger errors relative to sample size. The fractionation data for all the mafic grains show no resolvable effects and lie within the  $\pm 2$  per mil band. Similarly, no effects are observed in  $\delta^{26}\text{Mg}$ , and all the points, except one that has relatively large errors, lie within the  $\pm 2$  per mil band. The isotopic composition of the Mg in the mafic IDP's so far analyzed is therefore indistinguishable from that of terrestrial Mg.

**Spheres.** The first sphere analyzed showed a fractionation effect of 11 per mil per mass unit and a normal  $\delta^{26}\text{Mg}$  value (see Fig. 6). This is the first IDP sphere listed in Table 4. Two other spheres, chemically and morphologically similar to the first one (except for the difference in iron content) show no effects in either  $\Delta(^{25}\text{Mg}/^{24}\text{Mg})$  or  $\delta^{26}\text{Mg}$ . An SEM image of the anomalous sphere is shown in Fig. 4.

**Chondritic aggregates.** Four of these particles had Mg contents ranging from 2 ng to 80 pg. All have fractionation values within the normal range, but all except one show statistically significant ex-

cesses in  $\delta^{26}\text{Mg}$  ranging from 3.2 to 4 per mil. An SEM image of one of these anomalous particles is shown in Fig. 2.

All the data for the terrestrial standards and IDP's, with the exception of the fractionated Mg sphere, are shown in Fig. 7 as the measured raw  $^{25}\text{Mg}/^{24}\text{Mg}$  ratio versus the measured raw  $^{26}\text{Mg}/^{24}\text{Mg}$  ratio. Each data point represents the mean of a set of ten sequential ratios. In general, 15 to 20 such sets were obtained for each sample. The maximum scatter in  $^{25}\text{Mg}/^{24}\text{Mg}$  and  $^{26}\text{Mg}/^{24}\text{Mg}$  is  $\pm 3.5$  and  $\pm 7$  per mil, respectively. All the data are scattered around the mass fractionation line for normal Mg except the points for the fluffy aggregates, which are displaced from this line. It should be pointed out that the mean values given for each sample (see Table 4) are the statistical averages of 150 to 200 individual ratio measurements and the  $2\sigma$  mean errors show a much smaller spread than the range of scatter shown in Fig. 7. These results suggest that reliable data may be obtained by the direct-loading method to a precision of  $\sim \pm 1$  percent for samples containing  $\sim 10^{-12}$  g of Mg if it becomes possible to decrease laboratory contamination.

#### Calcium Analyses

It was previously demonstrated that for directly loaded samples, simultaneous beams of magnesium and calcium can be obtained (14, 15). The IDP's contain small amounts of Ca ( $\sim 1$  percent) and during the experiments described here large Ca beams ( $\sim 10^{-11}$  to  $5 \times$

$10^{-10}$  A) were observed during Mg runs. No attempt was made to investigate the optimum operating conditions or the long-term stability of Ca beams. However, some data for the three most abundant calcium isotopes,  $^{40}\text{Ca}$ ,  $^{42}\text{Ca}$ , and  $^{44}\text{Ca}$ , were obtained during three runs: two for samples of C-1 pyroxene ( $\sim 300$  pg of Ca) and one for a mafic particle (sample e in Table 4) containing 50 pg of Ca. All these samples gave raw  $^{40}\text{Ca}/^{44}\text{Ca}$  ratios between 46.0 and 46.7, which are indistinguishable from the terrestrial values under standard operating conditions to within 2 percent. After normalization for mass-dependent fractionation, all three samples had  $^{42}\text{Ca}/^{44}\text{Ca}$  ratios between 0.3098 to 0.3160, within  $\sim 1$  percent of the terrestrial value. The  $2\sigma$  mean error for the data ranged from about 2 percent for the C-1 pyroxene to about 4 percent for the IDP. The ionization efficiency for Ca was estimated to be  $\sim 0.1$ , which is a factor of 100 better than that obtained for large samples. It is clear that with some care, data on Ca and Mg in IDP's can be obtained simultaneously. A further investigation to determine the optimum operating conditions should improve the precision of the data substantially and extend the number of elements that can be analyzed by this method.

#### Orange and Green Lunar Spheres

Lunar green glass spheres from Apollo 15 and orange glass spheres from Apollo 17 were also analyzed. These samples were evidently formed as liquid droplets



and may have undergone substantial mass loss by volatilization. We analyzed samples of green and orange glass to search for possible fractionation effects in Mg. The data are listed in Table 4. The orange glass spheres show a normal Mg composition; fractionation and nonlinear effects are absent. The green glass spheres show no fractionation effects, but they appear to have negative values for  $\delta^{26}\text{Mg}$  ranging from  $-1.2$  to  $-2.0$  per mil (samples a, b, and c in Table 4). The statistical precision of the data is better than that of the IDP data as more material was available. However, previous analyses of macroscopic lunar samples did not show any evidence of Mg isotopic anomalies (21).

The negative  $\delta^{26}\text{Mg}$  values obtained for the lunar green spheres are puzzling. The  $-1.2$  to  $-2.0$  per mil deviation is close to the  $-1.5$  per mil offset that was observed for directly loaded samples with a higher Al content and was attributed to a reflected  $^{27}\text{Al}$  beam interfering with the  $^{24}\text{Mg}$  spectrum. However, the lunar green and orange spheres have a high Mg content and only small amounts of Al ( $\leq 2$  percent). In all cases the Al beam was sufficiently weak that no reflected beam was visible under the  $^{24}\text{Mg}$  peak. Furthermore, the orange spheres, which are chemically similar to the green spheres except for their high Ti content, do not show statistically significant deviations from zero in  $\delta^{26}\text{Mg}$ . Because of this problem, we analyzed terrestrial olivine with a low Al content. The data are listed in Table 4 and show no negative effects within the statistical accuracy quoted. In addition, some individual green glass balls were analyzed after chemical separation of Mg (d, e, f, and g in Table 4), and they also showed no clear evidence of a negative  $\delta^{26}\text{Mg}$ . The problem appears to be unresolved at present, and further studies will be needed to improve our understanding of the procedures for analysis by the direct-loading method at this level of precision. Because these deviations of up to 2 per mil in the lunar green glasses may be artifacts of the procedure, we infer that isotopic effects at the 2 per mil level may not be well defined by the experimental methods at their current stage of development. We must therefore conclude that the positive nonlinear effects observed for the chondritic aggregates at the level of 3 to 4 per mil are suggestive but not clearly established.

## Discussion

We have presented the first isotopic analyses of interplanetary dust particles.

These are considered to be different from meteoritic materials and are thought to represent samples of cometary debris. The overriding constraint during the investigation was the availability of only small amounts of material. It was demonstrated that individual samples as small as 5 to 10  $\mu\text{m}$  and weighing less than  $10^{-9}$  g can be reliably handled and analyzed. Techniques developed in this work permit isotopic analyses with  $10^{-10}$  g of Mg ( $3 \times 10^{11}$  atoms of  $^{26}\text{Mg}$ ) to a precision of 2 parts per thousand. Laboratory Mg contamination was typically 4 pg and comprises less than a few percent of the total Mg analyzed. The sensitivity achieved in mass spectrometric analysis for Mg is more than a factor of 100 better than that previously obtained.

The data for the IDP's can be summarized as follows: (i) the isotopic composition of the Mg in the mafic crystals is indistinguishable from that of terrestrial Mg, (ii) one of the spheres is fractionated by 11 per mil per mass unit, (iii) the chondritic aggregates show no fractionation effects and their isotopic compositions are very close to that of terrestrial Mg, (iv) three of the four chondritic aggregates have a statistically significant nonlinear anomaly near the limit of resolution, and (v)  $^{40}\text{Ca}$ ,  $^{42}\text{Ca}$ , and  $^{44}\text{Ca}$  abundances are the same as the terrestrial values within  $\sim 2$  percent in one IDP.

Data for the fractionated IDP sphere fall along a simple fractionation line for normal Mg; they are far outside the range of instrumental fractionation effects and the range of fractionation for terrestrial samples (see Fig. 6). We conclude that this grain was produced in a process that led to large isotopic fractionation. It is possible that the spherical shape of some of the IDP's is due to melting and ablation during atmospheric entry. The observed fractionation of 11 per mil could have been induced at this time by a distillation process, which would require loss by volatilization of more than 20 percent of the Mg in the particle. Two other IDP spheres that are similar in both morphology and chemistry to the fractionated sphere have a normal Mg isotopic composition. Furthermore, the lunar glass spheres do not show any fractionation effects. We infer that although the IDP sphere shows strong fractionation, a melting or volatilization process for small spherical particles does not, in general, produce significant isotopic separation.

The chondritic aggregates show no fractionation but have statistically significant positive values of  $\delta^{26}\text{Mg}$  ranging from 3.2 to 4 per mil with a typical  $2\sigma$  error of  $\sim 1$  per mil. The results of the analyses of EK1-4-1 spinel grains listed

in Table 2 show that nonlinear effects of the order of 3.5 per mil can be resolved, with the present techniques, for samples as small as  $10^{-10}$  g. However, measurements of lunar glass spheres indicate that it is possible to obtain shifts of  $\sim 2$  per mil by the direct-loading procedure that are absent in chemically separated samples. No peculiarities in either the operating conditions of the mass spectrometer or the mass spectra in the region of interest were observed during the experiments. Although convergence of the data for the chondritic aggregates to positive  $\delta^{26}\text{Mg}$  values is evident, it is possible that systematic effects due to the chemical composition of the particle can produce artifacts in the isotopic results at this level.

If the deviations from normal in the chondritic aggregates are real, it is not possible to state which isotopes are in anomalous abundance. The results could be explained by an excess of  $^{24}\text{Mg}$  or  $^{26}\text{Mg}$  or a deficiency of  $^{25}\text{Mg}$ . If the suggested effect is due to the decay of  $^{26}\text{Al}$ , this implies an extremely high initial  $^{26}\text{Al}/^{27}\text{Al}$  ratio of  $\sim 10^{-2}$  (8-10).

The mafic crystals are either single crystals or collections of a few large grains. They usually have clumps of chondritic material adhering to their surfaces that are similar in morphology and chemistry to the constituents of the IDP chondritic aggregates, implying a close association between the two types. However, the mafic crystals have a normal Mg isotopic composition and show no suggestion of either large fractionation or nonlinear isotopic effects.

In the continuing search for isotopic anomalies, there may be competition between relatively precise measurements on "large" samples and less precise measurements on small samples. For example, there is only a hint of isotopic effects in the IDP chondritic aggregates. The deviations in large ( $\sim 10 \mu\text{m}$ ) samples may be small (at the percent or per mil level) because the samples are aggregates of many primitive IDP's. It may therefore prove to be useful to investigate smaller ( $\sim 1 \mu\text{m}$ ) particles at a much lower level of precision, but with the possibility of finding large (tens of percent) effects undiluted by a collection of numerous dust particles that may average to normal isotopic composition.

Some of the difficulty in interpreting isotopic effects in both interplanetary dust and meteorites is that the parent bodies of the samples are unknown. Lunar samples are the only extraterrestrial materials that have been analyzed whose parent body is certain. In this regard, it would be highly desirable to obtain samples from a known comet. Short of a

spacecraft sample return mission, this might be accomplished by using aircraft to collect debris from a large meteor fireball having a cometary orbit, or by collecting debris from some of the intense cometary showers that occur several times a century. Further improvements in experimental techniques and the availability of larger quantities of IDP's can be expected to resolve more mysteries of the isotopic record that is preserved in early solar system debris.

#### References and Notes

1. J. S. Dohnanyi, in *Cosmic Dust*, J. A. M. McDonnell, Ed. (Wiley, London, 1978), p. 527; J. L. Weinberg and J. G. Sparrow, in *ibid.*, p. 75.
2. J. A. M. McDonnell, in *ibid.*, p. 337; F. L. Whipple, in *The Zodiacal Light and the Interplanetary Medium*, J. L. Weinberg, Ed. (SP-150, National Aeronautics and Space Administration, Washington, D.C., 1967), p. 409; P. M. Millman, in *Interplanetary Dust and Zodiacal Light*, H. Elsässer and H. Fechtig, Eds. (Springer, Berlin, 1976), p. 359.
3. D. E. Brownlee, in *Cosmic Dust*, J. A. M. McDonnell, Ed. (Wiley, London, 1978), p. 295; in *Protostars and Planets*, T. Gehrels, Ed. (Univ. of Arizona Press, Tucson, 1978), p. 135.
4. ———, D. A. Tomandl, E. Olszewski, in *Proceedings of the 8th Lunar Science Conference* (Lunar and Planetary Institute, Houston, 1977), p. 149.
5. J. G. Bradley, J. C. Huneke, G. J. Wasserburg, *J. Geophys. Res.* **83**, 244 (1978); I. D. Hutcheon, I. M. Steele, J. V. Smith, R. N. Clayton, in *Proceedings of the 9th Lunar and Planetary Science Conference* (Lunar and Planetary Institute, Houston, 1978), p. 1345.
6. G. J. Wasserburg, T. Lee, D. A. Papanastassiou, *Geophys. Res. Lett.* **4**, 299 (1977).
7. R. N. Clayton and T. K. Mayeda, *ibid.*, p. 295; T. Lee, D. A. Papanastassiou, G. J. Wasserburg, *Astrophys. J. Lett.* **220**, 21 (1978); M. T. McCulloch and G. J. Wasserburg, *ibid.*, p. 15; *Geophys. Res. Lett.* **5**, 599 (1978); D. A. Papanastassiou and G. J. Wasserburg, *ibid.* **4**, 595 (1977); G. W. Lugmair, K. Marti, N. B. Scheinin, in *Lunar and Planetary Science IX* (Lunar and Planetary Institute, Houston, 1978), p. 627.
8. T. Lee, D. A. Papanastassiou, G. J. Wasserburg, *Geophys. Res. Lett.* **3**, 109 (1976).
9. ———, *Astrophys. J. Lett.* **211**, 107 (1977).
10. J. C. Lorin, M. C. Michel-Lévy, *U.S. Geol. Surv. Open-File Rep. 78-701* (1978), p. 257.
11. J. D. Macdougall and D. Phinney, *Geophys. Res. Lett.* **6**, 215 (1979).
12. P. M. Millman, in *Nobel Symposium 21: From Plasma to Planet*, A. Elvius, Ed. (Wiley, New York, 1972), p. 157; *Naturwissenschaften* **66**, 134 (1979).
13. F. Tera and G. J. Wasserburg, *Anal. Chem.* **47**, 2214 (1975).
14. G. J. Wasserburg, T. Lee, D. A. Papanastassiou, *Lunar Science VIII* (Lunar Science Institute, Houston, 1977), p. 991.
15. T. Lee, D. A. Papanastassiou, G. J. Wasserburg, *Geochim. Cosmochim. Acta* **41**, 1473 (1977).
16. P. Fraundorf and J. Shirck, in *Proceedings of the 10th Lunar and Planetary Science Conference* (Lunar and Planetary Institute, Houston, in press).
17. R. S. Rajan, D. E. Brownlee, D. A. Tomandl, P. W. Hodge, H. Farrar, R. A. Britten, *Nature (London)* **267**, 133 (1977).
18. D. E. Brownlee, G. V. Ferry, D. Tomandl, *Science* **191**, 1270 (1976).
19. J. T. Armstrong and P. R. Buseck, *Anal. Chem.* **47**, 2178 (1975).
20. H. Y. McSween and S. M. Richardson, *Geochim. Cosmochim. Acta* **41**, 1145 (1977).
21. T. Lee, personal communication.
22. E. J. Catanzaro and T. J. Murphy, *J. Geophys. Res.* **71**, 1271 (1966).
23. This paper is dedicated to Fred Whipple, whose scholarship and passionate interest in comets and interplanetary dust have been a stimulus to many of us. Preliminary results of this work were presented at the 10th Lunar and Planetary Science Conference, Houston, 1979. This work was supported by NASA grant NGL 05-002-138 and NSF grant PHY76-83685. This is contribution 3293 (321) of the Division of Geological and Planetary Sciences, California Institute of Technology.

## AAAS-Newcomb Cleveland Prize

### To Be Awarded for an Article or a Report Published in *Science*

The AAAS-Newcomb Cleveland Prize is awarded annually to the author of an outstanding paper published in *Science* from August through July. This competition year starts with the 3 August 1979 issue of *Science* and ends with that of 25 July 1980. The value of the prize is \$5000; the winner also receives a bronze medal.

Reports and Articles that include original research data, theories, or synthesis and are fundamental contributions to basic knowledge or technical achievements of far-reaching consequence are eligible for consideration for the prize. The paper must be a first-time publication of the author's own work. Reference to pertinent earlier work by the author may be included to give perspective.

Throughout the year, readers are invited to nominate papers appearing in the Reports or Articles sections. Nominations must be typed, and the following information provided: the title of the paper, issue in which it was published, author's name, and a brief statement of justification for nomination. Nominations should be submitted to AAAS-Newcomb Cleveland Prize, AAAS, 1515 Massachusetts Avenue, NW, Washington, D.C. 20005. Final selection will rest with a panel of distinguished scientists appointed by the Board of Directors.

The award will be presented at a session of the annual meeting. In case of multiple authorship, the prize will be divided equally between or among the authors.